Draft version September 5, 2014
Preprint typeset using LaTeX style emulateapj v. 5/2/11

arXiv:1409.1473v1 [astro-ph.HE] 4 Sep 2014

HYPERCRITICAL ACCRETION, INDUCED GRAVITATIONAL COLLAPSE, AND BINARY-DRIVEN HYPERNOVAE

Chris L. Fryer[1], Jorge A. Rueda[2,3], Remo Ruffini[2,3]

Draft version September 5, 2014

ABSTRACT

The induced gravitational collapse (IGC) paradigm has been successfully applied to the explanation of the concomitance of gamma-ray bursts (GRBs) with supernovae (SNe) Ic. The progenitor is a tight binary system composed by a carbon-oxygen (CO) core and a neutron star (NS) companion. The explosion of the SN leads to *hypercritical* accretion onto the NS companion which reaches the critical mass, hence inducing its gravitational collapse to a black hole (BH) with consequent emission of the GRB. The first estimates of this process were based on a simplified model of the binary parameters and the Bondi-Hoyle-Lyttleton accretion rate. We present here the first full numerical simulations of the IGC phenomenon. We simulate the core-collapse and SN explosion of CO stars to obtain the density and ejection velocity of the SN ejecta. We follow the hydrodynamic evolution of the accreting material falling into the Bondi-Hoyle surface of the NS all the way up to its incorporation to the NS surface. The simulations go up to BH formation when the NS reaches the critical mass. For appropriate binary parameters the IGC occurs in short timescales $\sim 10^2 - 10^3$ s owing to the combined effective action of the photon trapping and the neutrino cooling near the NS surface. We also show that the IGC scenario leads to a natural explanation for why GRBs are associated only to SN Ic with totally absent or very little helium.

Subject headings: Type Ic Supernovae — Hypercritical Accretion — Induced Gravitational Collapse — Gamma Ray Bursts

1. INTRODUCTION

Continued observations of massive stars have demonstrated that most, if not all, massive stars are in binary systems (e.g. Smith et al. 2004; Kobulnicky & Fryer 2007; Sana et al. 2012, and references therein). A large fraction (50–75%) of these systems are in tight binaries that interact during the evolution (e.g. mass transfer, common envelope phase). The high binary fraction has led to a growing consensus that most type Ib/Ic supernova progenitors are produced in interacting binary systems (Podsiadlowski et al. 1992; De Donder & Vanbeveren 1998; Fryer et al. 2007; Yoon et al. 2010). Since the type of SNe associated to long-duration GRBs are of type Ic (Della Valle 2011), it is not surprising that binaries, often involving interactions of a massive star with a compact companion, have been invoked to produce GRB-SNe to remove the hydrogen envelope, spin up the star, or both (Fryer & Woosley 1998; Fryer et al. 1999c; Fryer & Heger 2005; van den Heuvel & Yoon 2007; Woosley & Bloom 2006; Fryer et al. 2007).

The *induced gravitational collapse* (IGC, Ruffini et al. 2008; Rueda & Ruffini 2012) model requires a tight binary (produced in a common envelope phase) between a massive CO star (a star that has lost its hydrogen envelope and helium shell) and a NS companion. In this scenario, the SN explosion and the GRB occur following a precise time sequence (see Fig. 1): explosion of the CO core → hypercritical accretion onto the NS → the critical mass is reached → gravitational collapse to a BH is induced → emission of the GRB. The theoretical framework and the first estimates of the hypercritical accretion onto the NS as a function of the nature of the binary parameters were first presented in (Rueda & Ruffini 2012).

It has been clear since the analysis of GRB 090618 by Izzo et al. (2012) that the entire emission of what has been traditionally called a GRB, instead of being a single event, is actually a *multiepisodic* source whose understanding needs a time-resolved data scrutiny data. The IGC has been successfully applied to a class of energetic ($E_{\rm iso} \sim 10^{52}$-10^{54} erg) GRB-SNe. These systems, recently named binary-driven hypernovae (BdHNe, Ruffini et al. 2014b), evolve in a rapid sequence lasting a few hundreds of seconds in their rest-frame. Up to now, the IGC has been verified in a dozen of GRBs, all with cosmological redshift $z \leq 1$ (see Pisani et al. 2013, and references therein), and very recently in one of the farthest observed sources, GRB 090423 at $z = 8.2$ (Ruffini et al. 2014c). These systems are characterized by four distinct episodes, each with specific signatures in its spectrum and luminosity evolution.

Episode 1: first part of the emission, it presents a soft X-ray spectrum with peak energies < 100 keV and is generally time-separated from the rest of the emission. It shows a complex spectrum which at times presents a thermal component. Physically, it has the imprint of the onset of the SN in a tight binary system with the companion NS. Its emission mainly originates from the hypercritical accretion, $\dot{M} \sim 10^{-2}\ M_\odot\ {\rm s}^{-1}$, of the SN ejecta onto the NS.

Episode 2: second part of emission observed with peak energies ∼ 100 keV–1 MeV. It is the canonical GRB emission originated from the gravitational collapse of the NS to a BH. The dynamics of the evolution of the highly relativistic (Lorentz factor $\Gamma \gtrsim 10^2$) e^+e- plasma, which engulfs baryonic matter and interacts with the circumburst medium (CBM), follows the fireshell model which takes into account the special relativistic effects and the plasma rate equation (see Ruffini 2011, and references therein).

Episode 3: the previously called *afterglow emission*, visible in optical, X-rays, and with a high energy component up to GeV energies, which observationally starts at the end of the GRB prompt emission. Independently from the features of the Episode 2 and its energetics, the Episode 3 appears to have a most remarkable scaling law and a universal behavior

[1] CCS-2, Los Alamos National Laboratory, Los Alamos, NM 87545
[2] ICRANet, P.zza della Repubblica 10, I–65122 Pescara, Italy
[3] Dipartimento di Fisica and ICRA, Sapienza Università di Roma, P.le Aldo Moro 5, I–00185 Rome, Italy

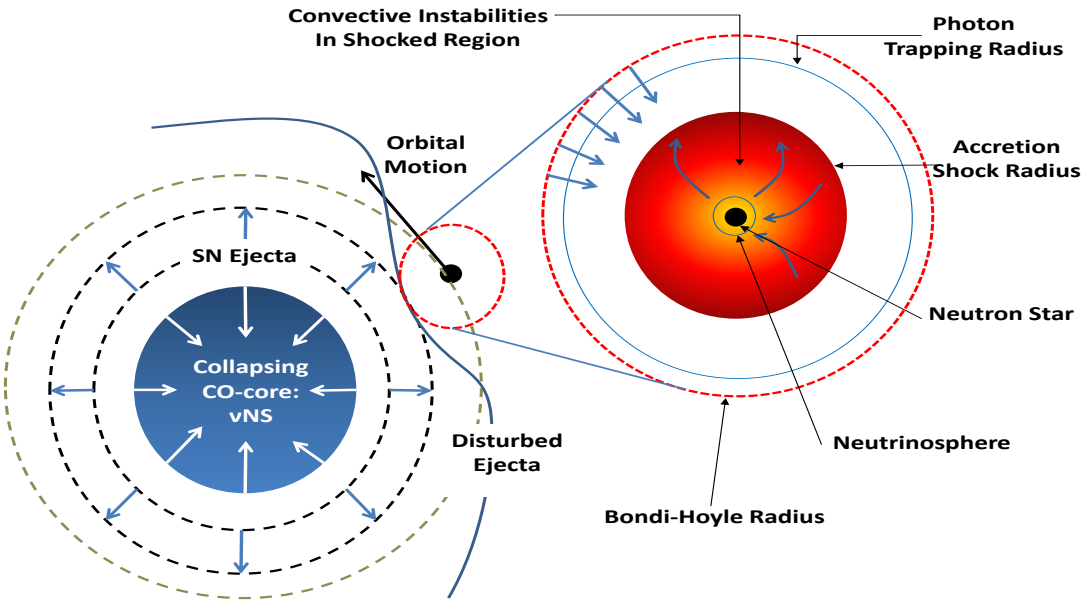

FIG. 1.— Induced gravitational collapse scenario.

for all the canonical GRBs. In the Swift-XRT lightcurve it consists, starting at the end of the GRB prompt, in a steep decay followed by a plateau and a late power-law decay (Pisani et al. 2013). The late X-ray luminosities of BdHNe, in their rest-frame energy band 0.3–10 keV, evidence a common power-law behavior, $L_X \propto t^{\alpha}$, with a constant decay index clustered around $\alpha = -1.5 \pm 0.2$. Such a constant afterglow decay represents an authentic nested structure (Ruffini et al. 2014b) in the late X-ray emission of GRB-SNe and it has been indicated as the qualifying feature for a GRB to be a BdHNe family member. The identification of GRB 090423 at $z = 8.2$ as a BdHN (Ruffini et al. 2014c) implies that SN events, leading to NS formation, can occur already at 650 Myr after the Big Bang. The above opens the way to consider the late X-ray power-law as a possible distance indicator.

Episode 4: emergence of the SN emission after $\sim$ 10–15 days from the occurrence of the GRB, in the source rest-frame. It has been observed for almost all the sources fulfilling the IGC paradigm with $z \sim 1$, for which current optical instrumentation allows their identification.

The first estimates of the IGC process (Rueda & Ruffini 2012; Izzo et al. 2012; Penacchioni et al. 2012, 2013; Pisani et al. 2013; Ruffini et al. 2013) were based on a simplified model of the binary parameters and the Bondi-Hoyle-Lyttleton accretion framework. The aim of this Letter is to better constrain the binary characteristics that lead to the IGC phenomenon (Episode 1) using more detailed supernova explosions coupled with models based on simulations of hypercritical accretion in supernova fallback (Fryer et al. 1996; Fryer 2009). We consider numerical simulations of collapsing CO cores leading to SN Ic in order to calculate realistic profiles for the density and ejection velocity of the SN outer layers. We follow the hydrodynamic evolution of the accreting material falling into the Bondi-Hoyle accretion region all the way up to its incorporation onto the NS surface.

2. BINARY PROGENITOR

The hypercritical accretion onto the NS from the SN ejecta in the IGC scenario can be estimated using the Bondi-Hoyle-Lyttleton formalism (Hoyle & Lyttleton 1939; Bondi & Hoyle 1944; Bondi 1952):

$$\dot{M}_{\rm BHL} = 4\pi r_{\rm BHL}^2 \rho (v^2 + c_s^2)^{1/2}\,, \quad (1)$$

where ρ is the density of the SN ejecta, v is the ejecta velocity in the rest frame of the NS (this includes a component from the ejecta velocity, $v_{\rm ej}$ and another component from the orbital velocity of the NS, $v_{\rm orb}$), c_s is the sound speed of the SN ejecta, and $r_{\rm BHL}$ is the Bondi radius:

$$r_{\rm BHL} = \frac{GM_{\rm NS}}{v^2 + c_s^2} \quad (2)$$

where G is the gravitational constant and $M_{\rm NS}$ is the NS mass. Both the velocity components, $v_{\rm orb}, v_{\rm ej}$, are typically much higher than the sound speed. The ejecta velocity as a function of time is determined by the explosion energy and the nature of the SN explosion. The orbital velocity depends upon the orbital separation, which in turn depends upon the radius of the CO star and the binary interactions creating the tight-orbit binary just prior to the explosion of the CO core. The effect of the NS magnetic field can be neglected for $\dot{M} > 2.6 \times 10^{-8}\ M_\odot\ {\rm s}^{-1} = 0.8\ M_\odot\ {\rm yr}^{-1}$ (Fryer et al. 1996; Rueda & Ruffini 2012)

The density evolution of the SN ejecta near the NS companion depends upon the SN explosion and the structure of the progenitor immediately prior to collapse. In Fig. 2, we show the density profile for three different low-metallicity stars with initial zero-age main sequence masses of $M_{\rm ZAMS}$ =15, 20, and 30 $M_\odot$ (Woosley et al. 2002). We designate the edge of the CO core in all of these stars. The density profile depends upon both on the initial conditions of the star (metallicity, initial mass, rotation) as well as the the stellar evolution code used (in this case, KEPLER). The density profile of a 20 $M_\odot$, solar metallicity star (Sam Jones, in preparation), is obtained using the MESA code. The IGC model assumes that both the hydrogen and helium layers are removed prior to collapse. There is a 3–4 order of magnitude pressure jump between the CO core and helium layer, indicating that the star will not expand significantly when the helium layer is removed. Comparisons of KEPLER models with the stripped CO cores from Moriya et al. (2010) suggest that, for some stellar evolution codes, the CO cores could be 1.5-2 times larger. We will discuss this

effect on the accretion rate below.

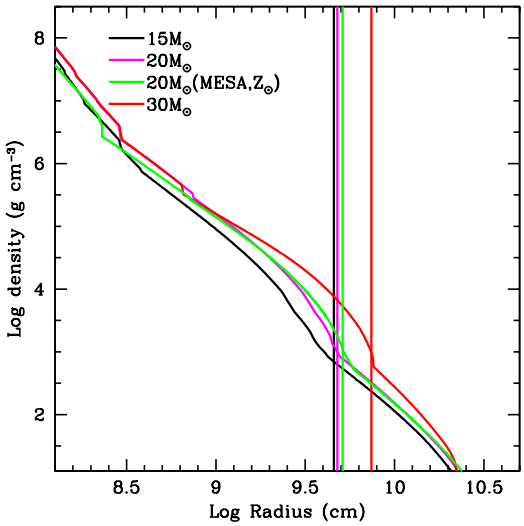

FIG. 2.— Density profile of different CO core progenitors with $M_{\rm ZAMS}$ =15, 20, and 30 $M_\odot$ for low-metallicity (Z=0.0001 $Z_\odot$) stars using the Kepler stellar evolution code (Woosley et al. 2002). For comparison, we include the density structure of a solar metallicity star produced by the MESA code (Sam Bond, in preparation). The vertical lines show the radius of the CO core. As we shall see below, the accretion rate is extremely sensitive to the structure of the star.

The compactness of the CO core (see Fig. 2) is such that there is no Roche lobe overflow[4] prior to the SN explosion. For instance, for a CO core progenitor with $M_{\rm ZAMS} = 15\ M_\odot$ ($M_{\rm CO} \approx 5\ M_\odot$, $R_{\rm CO} \approx 3 \times 10^9$ cm) no Roche lobe overflow occurs for binary periods $P \geq 2$ min, or binary separation $a \geq 6 \times 10^9$ cm, for a NS companion mass $M_{\rm NS} \geq 1.4\ M_\odot$.

3. BINARY DRIVEN HYPERCRITICAL ACCRETION

To derive the hypercritical accretion onto the NS, we must implement an explosion model. Here we take two approaches. The first is to assume a homologous outflow with a set explosion energy on the progenitor star structure. For comparison, we also use a second approach that follows the collapse, bounce, and explosion of the $20M_\odot$ progenitor discussed above using the parameterized model developed to study a range of SN explosion energies for fallback and SN light-curves (Frey et al. 2013). The calculation uses a 1D core-collapse code (Fryer et al. 1999a) to follow the collapse and bounce and then injects energy just above the proto-NS to drive different SN explosions mimicking the convective-engine paradigm. With this progenitor and explosion, we produce an example density and velocity evolution history at the position of the Bondi-Hoyle surface of our binary companion. Fig. 3 shows the Bondi-Hoyle infall rate from both our homologous outflow and our simulated SN models for a range of orbital separations (the innermost separation is determined to be just high enough so that the CO star does not overfill its Roche lobe). In our simulated explosion, the density piles up in the shock, producing a much sharper burst of accretion onto the NS. The accretion rate can be an order of magnitude higher in these models, but for a much shorter time such that the total mass accreted is only less than 2 times higher.

[4] The Roche lobe radius is (Eggleton 1983): $R_{\rm L,CO} \approx 0.49q^{2/3}/[0.6q^{2/3} + \ln(1+q^{1/3})]$, where $q = M_{\rm CO}/M_{\rm NS}$.

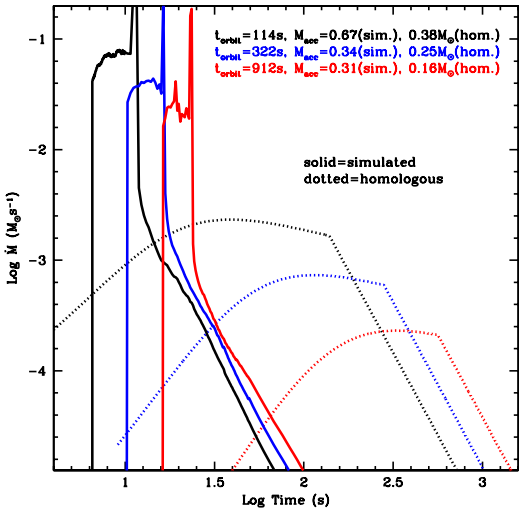

FIG. 3.— Hypercritical accretion for selected separation distances and for a star progenitor of 20 $M_\odot$ using our two approaches for the explosive engine. The supernova shock increases the density of the outgoing material, producing a pile up at the shock that leads to a spike in the accretion rate over a brief (few second) period, a much sharper accretion profile than our $\gtrsim 100$ s accretion time for our homologous outflow models.

This infall rate is well above the Eddington rate and will be reset to this rate if the assumptions of the Eddington accretion limit apply. The Eddington rate is derived assuming that the energy released when material accretes onto a compact object is released in photons and these photons exert pressure on the infalling material, reducing the accretion rate. The Eddington accretion limit, or critical accretion rate, makes a series of assumptions: the potential energy is released in the form of photons, the inflowing material and outflowing radiation is spherically symmetric, the photons are not trapped in the flow and can deposit momentum to the inflowing material, and the opacity is dominated by electron scattering. For a wide variety of accreting X-ray binaries, the Eddington limit seems to hold (at the order of magnitude level). But many of these assumptions break down for accretion rates as high as the ones achieved in the IGC scenario, hence hypercritical.

First and foremost, the photons in the hypercritical IGC accretion rates are almost certainly trapped in the flow. Chevalier (1989) derived the trapping radius where photons emitted diffuse outward at a slower velocity than infalling material flows inward:

$$r_{\rm trapping} = min[(\dot{M}_{\rm BHL}\kappa)/(4\pi c), r_{\rm BHL}] \quad (3)$$

where κ is the opacity (in cm^2 g^{-1}) and c is the speed of light. If the trapping radius is near or equal to the Bondi-Hoyle radius, the photons are trapped in the flow and the Eddington limit does not apply. This hypercritical accretion has been studied in detail for common envelope scenarios where κ is likely to be dominated by electron scattering. However, in SN fallback (Fryer et al. 1999b) and the IGC model, heavy elements are not completely ionized and lines can significantly increase the opacity. Following Colgan et al. (2013), we estimate for our CO core a Rosseland mean opacity roughly 5×10^3 cm^2 g^{-1}, a factor $\sim 10^4$ higher than electron scattering. This means that the trapping radius is higher for the IGC model. Combined with our high accretion rates, it is clear that the Eddington limit does not apply in this scenario and hypercritical, largely Super-Eddington accretion, occurs. The inflowing material shocks as it piles up onto the NS, producing an atmosphere on

TABLE 1
Hypercritical Accretion Mass in the IGC scenario

Progenitor ZAMS Mass	$M^a_{\rm acc}$ ($M_\odot$), $t_{\rm acc}$ (s) $a_{\rm orbit}/a^b_{\rm min}=1$	2	4	8
15 $M_\odot$	0.24, 160	0.15, 400	0.085, 600	0.042, 1300
20 $M_\odot$	0.38, 150	0.25, 250	0.16, 600	0.096, 1200
20 $M_\odot$[c]	0.67, 5	0.34, 6	0.31, 7	0.17, 7
20 $M_\odot$[d]	0.084, 150	0.058, 250	0.032, 600	0.001, 1200
30 $M_\odot$	0.62, 800	0.42, 2000	0.28, 3700	0.16, 8000

[a] Total accretion at super-Eddington rates in $M_\odot$.
[b] $a_{\rm min}$: minimum orbital separation such that the CO core does not fill its Roche lobe.
[c] Simulated with the KEPLER code.
[d] Solar metallicity star, simulated with the MESA code.

top of the NS (for details, see Zel'dovich et al. 1972; Chevalier 1989; Houck & Chevalier 1991; Fryer et al. 1996). As the atmosphere compresses, it becomes sufficiently hot to emit neutrinos which cool the infalling material, allowing it to be incorporated into the NS. For details of the simulation of this process, we refer the reader to (Ruffini & Wilson 1973; Fryer et al. 1996; Fryer 2009).

Table 1 shows the total mass accreted ($M_{\rm acc}$) for selected orbital separations and progenitor masses using different stellar evolution codes and different models (homologous vs. simulated) of the SN explosion. We also indicate the time interval ($t_{\rm acc}$) in which the accretion rate is integrated to obtain $M_{\rm acc}$. For these systems, the accretion rate is largely hypercritical exceeding 10^{-3} $M_\odot$ s^{-1}, so we expect a fraction of these systems to push beyond the maximum NS mass and collapse to a BH. Note that for the helium star systems, the accretion rate is not high enough to produce an IGC. If the radius of the CO core was twice that of our models (see discussion on the Moriya et al. (2010) models), our peak accretion rates would correspond to the $a_{\rm orbit}/a^b_{\rm min}=2$ values.

As material piles onto the NS and the atmosphere radius, the accretion shock moves outward. The accretion shock weakens as it moves out and the entropy jump (derived from the shock jump conditions) becomes smaller. This creates an atmosphere that is unstable to Rayleigh-Taylor convection. Simulations of these accretion atmospheres show that these instabilities can accelerate above the escape velocity driving outflows from the accreting NS with final velocities approaching the speed of light, ejecting up to 25% of the accreting material (Fryer et al. 2006; Fryer 2009). The entropy of the material at the base of our atmosphere, $S_{\rm bubble}$, is given by (Fryer et al. 1996):

$$S_{\rm bubble} = 38.7 \left(\frac{M_{\rm NS}}{2M_\odot}\right)^{7/8} \left(\frac{\dot{M}_{\rm BHL}}{0.1\ M_\odot {\rm s}^{-1}}\right)^{-1/4} \left(\frac{r_{\rm NS}}{10^6\ {\rm cm}}\right)^{-3/8} \quad (4)$$

k_B per nucleon, where $r_{\rm NS}$ is the radius of the NS. The corresponding temperature of the bubble, $T_{\rm bubble}$, is:

$$T_{\rm bubble} = 195\ S^{-1}_{\rm bubble} \left(\frac{r_{\rm NS}}{10^6\ {\rm cm}}\right)^{-1}. \quad (5)$$

For the typical hypercritical accretion conditions of the ICG, the temperature of the bubble when it begins to rise is $T_{\rm bubble}$ ~5 MeV. If it rises adiabatically, expanding in all dimensions, its temperature drops to 5 keV at a radius of 10^9 cm, far too cool to observe. However, if it is ejected in a jet, as simulated by Fryer (2009), it may expand in the lateral direction but not in the radial direction, so $\rho \propto r^2$ and $T \propto r^{-2/3}$. In this scenario, the bubble outflow would have $T_{\rm bubble} \sim 50$ keV at 10^9 cm and $T_{\rm bubble} \sim 15$ keV at 6×10^9 cm. This could explain the temperature and size evolution of the blackbody emitter observed in the Episode 1 of several BdHNe (Izzo et al. 2012; Penacchioni et al. 2012, 2013; Pisani et al. 2013; Ruffini et al. 2013, see, e.g.,). For instance, the blackbody observed in Episode 1 of GRB 090618 (Izzo et al. 2012) evolves as $T \propto r^{-m}$ with $m = 0.75 \pm 0.09$, whose lower value is in striking agreement with the above simplified theoretical estimate. We are currently deepening our analysis of the possible explanation of the thermal emission observed in Episode 1 of BdHNe as due to the convective instabilities in the accretion process. However, this is out of the scope of this work and the results will be presented elsewhere.

4. DISCUSSION

While in this Letter we address simulations of the Episode 1 of the IGC, let us shortly outline some recent progress in the understanding the structure of Episode 3 which may become complementary to this work: a) the remarkable scaling laws in the X-ray luminosity in all BdHNe (see Pisani et al. 2013; Ruffini et al. 2014b, for details); b) the very high energy emission, all the way up to 100 GeV in GRB 130427A, as well as the optical one, follow a power-law behavior similar to the X-ray emission described above. The corresponding spectral energy distribution is also described by a power-law function with quite similar decay indexes (Ruffini et al. 2014a). These results clearly require a common origin for this emission process; c) an X-ray thermal component has been observed in the early phases of the Episode 3 of GRBs 060202, 060218, 060418, 060729, 061007, 061121, 081007, 090424,100316D, 100418A, 100621A, 101219B and 120422A (Page et al. 2011; Starling et al. 2012; Friis & Watson 2013). This feature has been clearly observed in GRB 090618 and GRB 130427A, implying a size of the emission region of 10^{12}–10^{13} cm expanding at velocity $0.1 < v/c < 0.9$, hence a bulk Γ Lorentz factor $\lesssim 2$ (Ruffini et al. 2014b,a).

Recently, Ruffini et al. (2014b) raised the possibility of using the nuclear decay of ultra-heavy r-process nuclei, originated in the close binary phase of Episode 1, as an energy source of the Episode 3. These processes lead to a power-law emission (see, e.g., Kasen et al. 2013) with decay index similar to the one observed in Episode 3. The total energy emitted in the nuclear decays is also in agreement with the observations in the Episode 3 of BdHNe. r-process avalanches in BdHNe could also originate from a similar mechanism as the one outlined by Fryer et al. (2006) in SN fallback. An additional possibility to generate the scale-invariant power-law in the luminosity evolution and spectrum are the type-I and type-II Fermi acceleration processes (Fermi 1949) during the evolution of the SN remnant. The application of the Fermi acceleration mechanisms has two clear advantages; the generation of the aforementioned power-law behaviors, and to solve the longstanding problem formulated by Fermi of identifying the injection source to have his acceleration mechanism at work at astrophysical scales.

We have advanced our estimates of the NS accretion rate within the IGC model, which leads to BdHNe with all the above features. Our estimates assume that the Bondi-Hoyle-Lyttleton formalism is valid for our calculations. Although it has been shown that this formalism is valid in steady-state systems (see Edgar 2004, and references therein), the IGC model, with its time-variable conditions may push the validity of these assumptions. Full accretion models are required in order to validate our results and/or to produce more reliable accretion rates.

It appears from observations that a necessary condition to produce a GRB-SN is that the pre-SN core is fully absent of

or has very little helium. We have shown that the IGC process provides a natural explanation for that condition: hypercritical accretion rates are favored by the presence of a compact CO core since it leads to tighter binaries and produces higher opacities of the ejecta which favors the photon trapping. We showed that helium cores do not trigger enough hypercritical accretion onto the NS companion to produce an IGC. A number of mechanisms have been proposed to remove this material (a common problem for most GRB scenarios): stellar winds (the difficulty with this model is removing just the helium layer and not a considerable portion of the CO core), mass transfer (only low-mass helium cores undergo a helium giant phase, so conditions for mass transfer or common envelope phases may be difficult to reproduce), enhanced mixing allow fusion to consume the helium layer (Frey et al. 2013). Detailed simulations of the binary evolution up to the formation of binary systems conforming with the IGC conditions are needed in order to assess this fundamental question.

REFERENCES

Bondi, H. 1952, MNRAS, 112, 195
Bondi, H., & Hoyle, F. 1944, MNRAS, 104, 273
Chevalier, R. A. 1989, ApJ, 346, 847
Colgan, J., Kilcrease, D. P., Magee, N. H., et al. 2013, High Energy Density Physics, 9, 369
De Donder, E., & Vanbeveren, D. 1998, A&A, 333, 557
Della Valle, M. 2011, International Journal of Modern Physics D, 20, 1745
Edgar, R. 2004, New Astronomy Reviews, 48, 843
Eggleton, P. P. 1983, ApJ, 268, 368
Fermi, E. 1949, Phys. Rev., 75, 1169
Frey, L. H., Fryer, C. L., & Young, P. A. 2013, ApJL, 773, L7
Friis, M., & Watson, D. 2013, ApJ, 771, 15
Fryer, C. L. 2009, ApJ, 699, 409
Fryer, C. L., Benz, W., & Herant, M. 1996, ApJ, 460, 801
Fryer, C. L., Benz, W., Herant, M., & Colgate, S. A. 1999a, ApJ, 516, 892
Fryer, C. L., Colgate, S. A., & Pinto, P. A. 1999b, ApJ, 511, 885
Fryer, C. L., & Heger, A. 2005, ApJ, 623, 302
Fryer, C. L., Herwig, F., Hungerford, A., & Timmes, F. X. 2006, ApJL, 646, L131
Fryer, C. L., & Woosley, S. E. 1998, ApJL, 502, L9
Fryer, C. L., Woosley, S. E., & Hartmann, D. H. 1999c, ApJ, 526, 152
Fryer, C. L., Mazzali, P. A., Prochaska, J., et al. 2007, PASP, 119, 1211
Houck, J. C., & Chevalier, R. A. 1991, ApJ, 376, 234
Hoyle, F., & Lyttleton, R. A. 1939, Proceedings of the Cambridge Philosophical Society, 35, 405
Izzo, L., Ruffini, R., Penacchioni, A. V., et al. 2012, A&A, 543, A10
Kasen, D., Badnell, N. R., & Barnes, J. 2013, ApJ, 774, 25
Kobulnicky, H. A., & Fryer, C. L. 2007, ApJ, 670, 747
Moriya, T., Tominaga, N., Tanaka, M., et al. 2010, ApJ, 719, 1445
Page, K. L., Starling, R. L. C., Fitzpatrick, G., et al. 2011, MNRAS, 416, 2078
Penacchioni, A. V., Ruffini, R., Bianco, C. L., et al. 2013, A&A, 551, A133
Penacchioni, A. V., Ruffini, R., Izzo, L., et al. 2012, A&A, 538, A58
Pisani, G. B., Izzo, L., Ruffini, R., et al. 2013, A&A, 552, L5
Podsiadlowski, P., Joss, P. C., & Hsu, J. J. L. 1992, ApJ, 391, 246
Rueda, J. A., & Ruffini, R. 2012, ApJL, 758, L7
Ruffini, R. 2011, International Journal of Modern Physics D, 20, 1797
Ruffini, R., Bernardini, M. G., & Bianco et al., C. L. 2008, in The Eleventh Marcel Grossmann Meeting, ed. H. Kleinert, R. T. Jantzen, & R. Ruffini, 368–505
Ruffini, R., & Wilson, J. 1973, Physical Review Letters, 31, 1362
Ruffini, R., Izzo, L., Muccino, M., et al. 2013, ArXiv:1311.7432
Ruffini, R., Wang, Y., Kovacevic, M., et al. 2014a, ArXiv e-prints
Ruffini, R., Muccino, M., Bianco, C. L., et al. 2014b, A&A, 565, L10
Ruffini, R., Izzo, L., Muccino, M., et al. 2014c, ArXiv:1404.1840
Sana, H., de Mink, S. E., de Koter, A., et al. 2012, Science, 337, 444
Smith, N., Morse, J. A., Collins, N. R., & Gull, T. R. 2004, ApJL, 610, L105
Starling, R. L. C., Page, K. L., Pe'Er, A., Beardmore, A. P., & Osborne, J. P. 2012, MNRAS, 427, 2950
van den Heuvel, E. P. J., & Yoon, S.-C. 2007, Ap&SS, 311, 177
Woosley, S. E., & Bloom, J. S. 2006, ARA&A, 44, 507
Woosley, S. E., Heger, A., & Weaver, T. A. 2002, Reviews of Modern Physics, 74, 1015
Yoon, S.-C., Woosley, S. E., & Langer, N. 2010, ApJ, 725, 940
Zel'dovich, Y. B., Ivanova, L. N., & Nadezhin, D. K. 1972, Soviet Astronomy, 16, 209